AIAA JOURNAL
Vol. 46, No. 1, January 2008

Design of Optimized Patches to Reinforce Damaged Wings

Jean-Denis Mathias,* Michel Grédiac,† and Xavier Balandraud‡
Laboratoire de Mécanique et Ingénieries,
63175 Aubière, France

DOI: 10.2514/1.24300

This paper describes the optimization process of composite patches designed to reinforce damaged wings. The main objective is to reduce the stress level in a damaged area located near the anchorage of the wing to the fuselage. Genetic algorithms are used for optimizing the ply orientations of the stacking sequence as well as the location and shape of the patch. The stress field in the structure is computed with the ANSYS finite element package. Several examples illustrate the fact that the stress flow within the wing is deviated, thus leading to a decrease of the stress level in the damaged area to be relieved.

I. Introduction

COMPOSITE patches have been used to repair aeronautical structures since the 1970s [1–3]. These patches are mainly used to bridge cracks, thus limiting their expansion throughout the structure and increasing the residual lifespan for up to several years. Typical technical solutions are described in detail in [4].

A similar approach consists of reinforcing aeronautical structures before defects appear. In this case, some zones of the structures are damaged but cracks have not yet appeared, and the goal is to delay crack appearance. Reinforcement can be obtained by bonding an additional material (namely a patch) on the structure in such a way that the stress level in the damaged zone decreases. Crack appearance is therefore expected to be delayed. It must be underlined that when stress is decreased by a few percent, it may significantly delay crack appearance and therefore significantly expand the residual life of the damaged structure, as can be easily checked on typical Wholer's curves.

The determination of the patch characteristics in terms of shape, ply orientation, location, and constitutive material is an important issue. In particular, one can either directly bond the patch on the damaged area, as in the case of crack bridging, or bond it outside this zone. One can expect a local stiffness increase in the first case and therefore a stress relief in the metallic substrate just beneath the patch. In the second case, the patch may deviate the stress flow from the damaged zone. For a given patch surface, the issue is to know which of the two solutions is the most efficient. This study tackles the preceding issues using a genetic algorithm (GA) and a finite element (FE) program. The former performs the optimization of the shape, stacking sequence, and location of the patch, whereas the latter computes the stress field within the structure.

In this paper, the foundations of GAs are first recalled . The main genetic operators are then described in the context of wing reinforcement. The relevancy of the approach is illustrated through a typical problem of wing reinforcement. Solutions provided by the procedure are finally discussed.

Received 28 March 2006; accepted for publication 28 August 2007.

*Corresponding author. Campus des Cézeaux, BP 265; currently Professor Assistant, Cemagref, Unité de Recherche, Laboratoire d'Ingénierie des Systémes Complexes, 24 Avenue des Landais, BP 20085, F-63172 Aubiére, France; jean-denis.mathias@cemagref.fr.

†Professor, Laboratoire de Mécanique et Ingénierie (Université Blaise Pascal/Institut Français de Mécanique Avancée), 24 Avenue des Landais, BP 20085, F-63172 Aubiére, France.

‡Professor Assistant, Laboratoire de Mécanique et Ingénierie (Université Blaise Pascal/Institut Français de Mécanique Avancée), 24 Avenue des Landais, BP 20085, F-63172 Aubiére, France.

II. Optimization by Genetic Algorithms

A. Introduction

An overview of the literature dealing with composite structure optimization shows that GAs can be advantageously used for solving this type of problem [5–10]. One of the features of composite material optimization problems is the fact that functions to be minimized depend on discrete variables such as ply angles or number of plies, thus leading classical first- or second-order optimization methods to be unsuitable. Another feature is that objective functions involved in this case often exhibit several local optima [11]. GAs are well adapted for solving this type of optimization problem. In addition, they provide a large population of potential solutions contrary to traditional optimization methods, which generally provide a single solution only. Further choices among the population are then possible, thus enabling the designer to perform a more refined analysis of the results.

A preliminary work dealing with the reinforcement of simple structures such as holed metallic specimens under tensile loading has been recently carried out [12]. It has shown the suitability of GAs for solving simple reinforcement problems. The objective here is to push forward the idea by examining the reinforcement of a much more complicated structure: a typical wing. This tool will be used to solve some design problems such as the choice of the constitutive material, the determination of the stacking sequence and the shape of the patch. The optimal choice of patch shape is seldom addressed in the literature [13], for instance. In this latter study, usual shapes only are considered: square, circle, or ellipse. Moreover, it deals with the repair of cracked structures and not with the preventive reinforcement of existing structures in which no cracks have appeared. The aim of the current work is to underline that the shape of the patch significantly influences the efficiency of the reinforcement. It must finally be underlined that the present paper does not deal with the optimization of the initial design of aeronautical structure, but with the optimization of the reinforcement of preexisting structures. GAs have proven to be a very powerful and flexible tool to solve the first type of problem (see [14–18], for instance), and so the idea here is to use the same tool to optimize composite patches used for reinforcement purposes. The wing itself cannot be modified to avoid ensuing problems such as fuel tank location, flutter characteristics, or the dynamic response.

B. Definition of the Problem

Let us consider the schematic view of a wing shown in Fig. 1. Its shape is similar to that of a Dassault–Dornier "Alphajet" used as training jet in the French air force. It is embedded to the fuselage along its right-hand side. Actual wings are boxed structures which exhibit nine stiffeners, four ribs, one lower surface, and one upper surface. In the present study, constructing a three-dimensional model of such a type of structure is not realistic because of the numerous calculations performed during the optimization process. As a result, a

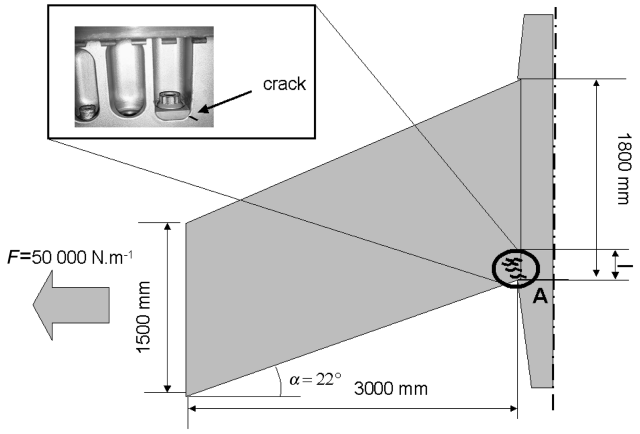

Fig. 1 Geometry of the wing.

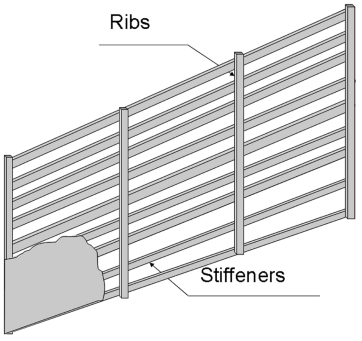

Fig. 2 Ribs and stiffeners.

two-dimensional model of a lower surface subjected to a tensile loading is considered (see Fig. 2). For the sake of simplicity, the wing is subjected here to a tensile loading along the left-hand side of the border. The stress level is the highest in zone A (see Fig. 1) where cracks appear near the bolt. It must be emphasized that this stress distribution is similar to the actual stress distribution within the Dassault–Dornier Alphajet wing. Results obtained are consistent with the fact that, in practice, fatigue cracks actually appear in the zone where the highest stress level takes place (zone A in Fig. 1). The present problem can then be considered as a first simplified study carried out to analyze the effect of a patch on the stress redistribution in a damaged wing.

As explained in the preceding section, the objective here is to find the location, the shape, and the stacking sequence of a composite patch so that this stress level in zone A is reduced. This stress level could be estimated with a global criterion such as the von Mises or the Dang Van criteria [19] which would be suitable in the cases of static and fatigue loadings, respectively. The requirement of the lowest stress level in zone A is transformed into the highest reduction of the force applied by the wing to the fuselage along the first eighth of the right-hand border (see Fig. 1). It has been observed that the results obtained only slightly depend on this length which is denoted l in the following. Reducing the force along this portion of line directly leads to a reduction of the stress level in zone A because this zone is in the vicinity of this portion of line.

The stress throughout the structure is computed using the finite element package ANSYS. The main assumption is the fact that the wing is considered a two-dimensional structure which is therefore meshed with suitable two-dimensional elements such as SHELL93 eight-noded quadrilaterals. Stiffeners and ribs are modeled with two-noded BEAM4 elements. The two-dimensional analysis does not take into account the membrane/bending coupling which would result from the asymmetry of the model. Bonding between patch and substrate is supposed to be perfect by merging nodes of the elements used to mesh the patch and the substrate. Out-of-plane stress components cannot be calculated because of the bidimensional nature of the model. In particular, this assumption means that the out-of-plane shear stress components in the adhesive are not computed. The progressive load transfer between substrate and patch [20] is also ignored. These phenomena could, however, be easily studied using a three-dimensional postprocessor.

C. Optimization Problem

The optimization problem is written as follows:
Minimize

$$f(\boldsymbol{V}) \tag{1}$$

subjected to

$$g_i \leq 0; \qquad i = 1, n_g \tag{2}$$

$$L_j \leq v_j \leq U_j; \qquad i = 1, n_v \tag{3}$$

where $\boldsymbol{V}$ is the vector of design variables, f is the objective function to be minimized, g_i are the constraints of the structural optimization problem, n_g is the number of constraints, L_j and U_j are, respectively, the lower and the upper limits of variables v_j, and n_v is the number of variables.

In the present problem, the design variables are the n-ply orientations as well as the geometry and the location of the patch. More details on these variables are as follows:

1) Ply orientations $[\theta_1, \theta_2, \ldots, \theta_n]$ are modeled by discrete variables which can only be equal to 0, −45, 45, and 90 deg for some practical reasons. The composite patch is here made of six plies. An angle denoted β enables one to define the global orientation of the patch with respect to the wing (see Fig. 3).

2) A closed plane spline curve is used to describe the boundary of the patch (see Fig. 3). This curve is described by height interpolation points whose coordinates are considered as design variables in the optimization problem. Preliminary calculations have shown that choosing eight interpolation points is a good compromise between shape diversity and simplicity in the definition of the boundary. A specific procedure avoiding any loop in the curve has been developed. This procedure is described in detail in [12]. It is therefore not recalled here.

As a result, the optimization problem depends on 23 variables in this first approach: six ply orientations, one global orientation of the patch, and 16 coordinates of the eight interpolation points which define the spline curve. The variables are represented in Fig. 4, in which the details on the chromosome representing each individual are given. The optimization is performed under a constraint which is the maximum allowable surface of the patch denoted A_p. It is a given percentage of the surface of the wing denoted A_w. The influence of

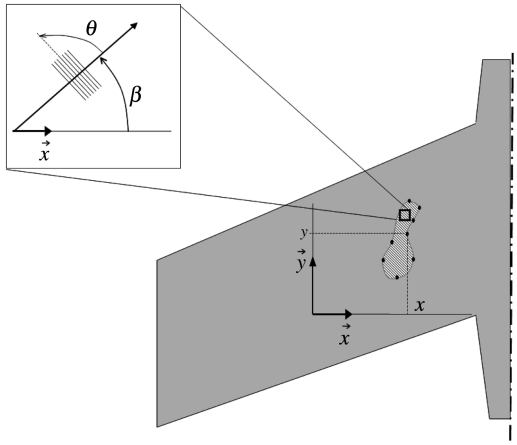

Fig. 3 Design variables: (x, y) are the coordinates of the interpolation points, θ the ply orientations, and β global orientation with respect to the x direction.

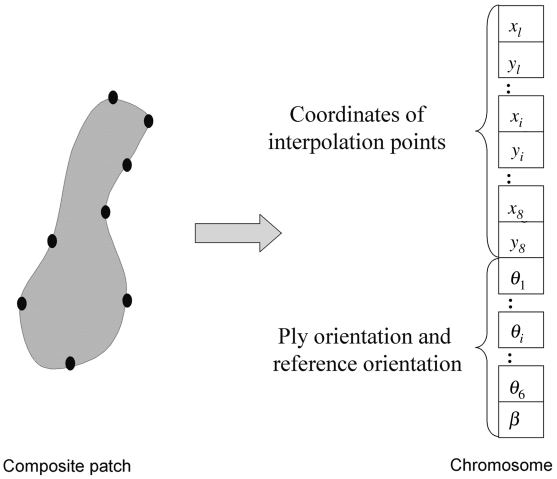

Fig. 4 Chromosome of patch variables: 16 genes encode the coordinates of the interpolation points, seven genes encode the ply orientations and the global reference.

the percentage on the efficiency of the reinforcement is discussed in Sec. IV.C.

Objective function f is defined by the force applied by the wing on the fuselage along l. It is defined by

$$f = \sum_{k}^{n_a} \|F\|_k \tag{4}$$

where n_a corresponds to the number of nodes distributed along l. The corresponding fitness G is defined by

$$G = C - f \tag{5}$$

where C is a constant small enough to enable a good comparison between individuals of a given generation and large enough to avoid negative values of the fitness. In practice, C is defined by

$$C = f_{\max} \tag{6}$$

where $f_{\max}$ corresponds to the objective function of the worst individual at each generation as suggested in [21]. G is therefore defined by:

$$G = \sum_{k}^{n_a} \|F\|_k^{(\mathrm{wi})} - \sum_{k}^{n_a} \|F\|_k \tag{7}$$

The sum $\| F\|_k^{(\mathrm{wi})}$ corresponds to the sum of the worst individual. In practice, f is minimized by maximizing G with the GA.

D. Genetic Operators

Two selection operators are used to select parents:

1) The elitist selection, which consists in keeping the best individuals of a generation in the next generation, ensures the convergence of the algorithm.

2) The proportional selection which eliminates individuals depending on their survival probability P^S is defined by

$$P^S = \frac{G}{\sum_{i=1}^{n} G(i)} \tag{8}$$

where n is the number of individuals of the current population. Best individuals are favored but a chance is also given to the weakest ones.

After parent selection, a real crossover is applied to the coordinates of the spline curve and to the global orientation β. Let g_{p1} and g_{p2} be the parent genes of the patch. The corresponding child genes g_{c1} and g_{c2} of the two children are defined by

$$\begin{cases} g_{c1} = \omega \times g_{p1} + (1-\omega) \times g_{p2} \\ g_{c2} = \omega \times g_{p2} + (1-\omega) \times g_{p1} \end{cases} \tag{9}$$

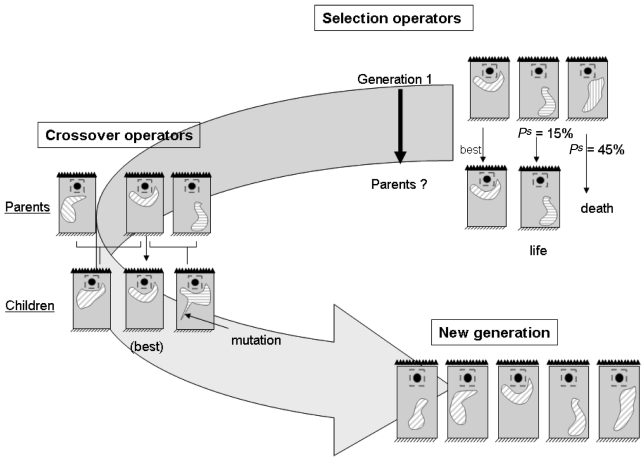

Fig. 5 Schematic view of the optimization procedure.

where ω is a parameter randomly lying between zero and one to preserve the feasibility of the solution. Indeed, it has been observed that choosing $\omega > 1$ or $\omega < 0$ often leads to patches which exhibit some parts located outside the structure to be relieved, which means that Eq. (3) is not satisfied. Individuals are finally exposed to mutation after crossover. The mutation operator randomly modifies the gene values of the children with a mutation probability P_m which is equal here to 0.01.

Two additional operators have been used in the optimization procedure:

1) A local improvement can be advantageously used to increase the convergence of the program, as pointed out in [22], for instance. It consists of small changes in each gene of the best individual to try to obtain a better solution. One addition and one subtraction affecting each variable are successively tested. If a better solution is found, it is kept in the next generation. As a result, if the best solution exhibits n_v genes, $2 \times n_v$ individuals (n_v additions and n_v subtractions) are tested with the local improvement.

2) A new operator is introduced to complete the local improvement: a translation operator. It consists in translating the best patch at each generation in four directions: x, $-x$, y, and $-y$. The amplitude of this translation is equal to the pitch of the regular mesh used in the FE program.

If one of the preceding $2 \times n_v + 4$ individuals is better than the best individual of the current generation, it is kept in the next generation to perform the elitist selection. Figure 5 represents the main steps governing the evolution of the population. In practice, the initial population size is equal to 160 individuals. Some preliminary calculations have shown that this choice is reasonable [12].

III. Example

A. Modeling

As explained in Sec. II.B, the model is bidimensional for the sake of simplicity. It is considered as an aluminum plate (4 mm in thickness). Mechanical properties are those of a 2024 T3 aluminum. The patch is a six-ply stacking sequence made of unidirectional carbon–epoxy plies. The thickness of each ply is 0.25 mm. This uniform thickness is chosen because of some industrial constraints. The mechanical properties of these two materials are reported in Table 1. Stiffeners and ribs are modeled with beams whose moment of inertia is 1500 mm [4]. Common nodes of beams and plate are

Table 1 Mechanical properties of the materials

	Carbon–epoxy	Boron–epoxy	Aluminum
E_x, GPa	141	200	72
E_y, GPa	10	10	——
ν_{xy}	0.28	0.3	0.32
G_{xy}, GPa	7	10	——

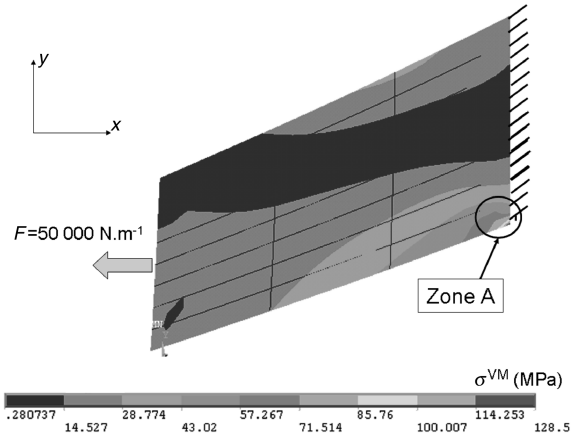

Fig. 6 Von Mises stress distribution in the wing without patch.

merged to model perfect bonding between both types of substructures.

The diversity of patch geometries is broad to guarantee an unbiased optimization procedure. In addition, the same element size and regular mesh are chosen for all individuals to avoid any influence of the mesh density. As a result, the spline curve modeling the boundary of the patch is not smooth because it is also discretized with the same density as the mesh. Some preliminary calculations have been carried out to choose the mesh density. This density has been chosen to obtain a good compromise between the accuracy of the results and the calculation time.

B. Stress Field in the Unreinforced Wing

Figure 6 represents the von Mises stress distribution in the wing subjected to the loading shown in Fig. 1. This stress map shows significant stresses at the anchorage of the wing. It corresponds to the actual location of the damage appearance in the Alphajet.

The sum of forces collected at the nodes located along l is equal to $f_{\text{ref}} = 71,880$ N. This sum is considered hereafter as the reference force which has to be reduced by bonding composite patches on the wing.

C. Optimized Patches

Figure 7 represents different optimized patches obtained using the aforementioned procedure in the case of a maximum allowable maximum patch surface equal to 20% of the wing's surface. The computation time is about one day with a 3.06 GHz Pentium 4 computer. The GA generally converges after 10 generations. Figure 8 represents a typical convergence plot of the GA. The interpolation point coordinates of the best patch are

$$\begin{aligned} x^{p1} &= 2100 y^{p1} = 2400 & x^{p2} &= 1950 y^{p2} = 1950 \\ x^{p3} &= 3000 y^{p3} = 1500 & x^{p4} &= 2850 y^{p4} = 1950 \\ x^{p5} &= 2250 y^{p5} = 1950 & x^{p6} &= 2550 y^{p6} = 1500 \\ x^{p7} &= 3000 y^{p7} = 1650 & x^{p8} &= 2550 y^{p8} = 2850 \end{aligned} \tag{10}$$

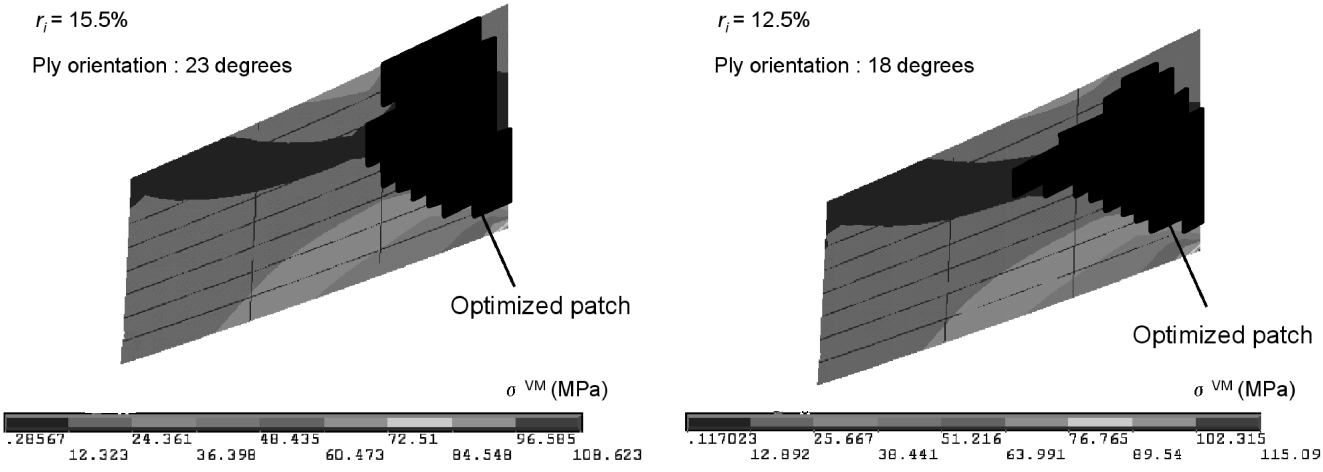

a) First optimized patch **b) Second optimized patch**

Fig. 7 Von Mises distributions of optimized patch and ply orientation with respect to the x direction.

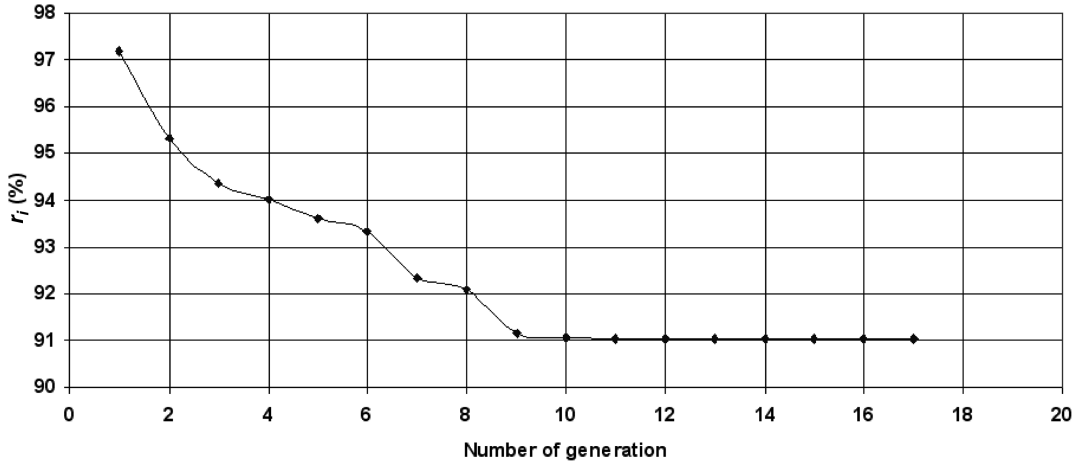

Fig. 8 Convergence curve of the genetic algorithm.

The suitability of any solution i is rated with r_i which is defined as follows:

$$r_i = 1 - \frac{f_i}{f_{\text{ref}}} \tag{11}$$

where f_i is the sum of the forces collected at the nodes along l in the FE model of solution i. Ratio r_i directly represents the force drop along l after bonding the patch. The highest r_i, the highest fitting. The rating of the best patch is 15.5%. It must be underlined that reducing by 15.5% the stress level in the wing may significantly increase the lifespan of the structure. As can be seen in Fig. 7, the composite patch slightly deviates the stress flow toward the upper part of the wing to relieve its lower part. It is interesting to note that the upper part of the wing is overloaded because the lower one is underloaded. It can be checked, however, that this higher stress level at the top does not significantly decrease the lifespan of this part of the wing. Ply orientations are defined by a global orientation $\beta = 23$ deg and six 0 deg plies. The stiffener angle is slightly higher than β (approximately 30 deg). This value seems reasonable because the fibers are expected to be more or less aligned with the direction of the stiffeners. All patches found exhibit one fiber orientation only, even though each ply is allowed to rotate independently from each other during the optimization process. This shows that a unidirectional patch is the most efficient to deviate the stress flow from zone A in Fig. 1. It is clear that some additional constraints such as bucking load, flutter speed, or airflow around the reinforced wing should be studied in detail. Adding such constraints in the cost function which is minimized seems, however, difficult, and these issues should be tackled a posteriori on the optimized solution provided by the program.

The GA has been launched with different initial populations. It has converged to optimized patches which are nearly the same as the optimized patches presented in Fig. 7. And so, in this case, this solution is validated to reinforce the wing.

D. Comparison with a Rectangular Patch

Rectangular patches are used in several studies dealing with structural repair [1,23,24]. In the current study, to highlight the sensitivity of the stress relief to both the fiber orientation and the shape of the patch, the preceding result can be compared with the ratio r_i obtained with a rectangular unidirectional patch bonded at the upper right-hand side corner of the structure. In this case, the fiber direction is 0 deg and the patch exhibits the same surface A_p as in the preceding case: $A_p = A_w \times 20\%$. The ratio obtained here is more than three times lower as in the preceding section: $r_i = 4.7\%$ instead of $r_i = 15.5\%$. This result clearly highlights the very positive effect of adjusting ply orientation and patch shape. It also illustrates the interest of the present approach from a design point of view.

IV. Sensitivity Analysis

A. Introduction

The aim of this section is to modify the following parameters governing the problem and to observe their influence on the ratings found:

1) Influence of the constitutive material: In [25], for instance, patches used for repairing aircraft are made in boron–epoxy. Hence, some simulations have been performed with this material. Isotropic patches have also been tested to highlight the influence of anisotropy.

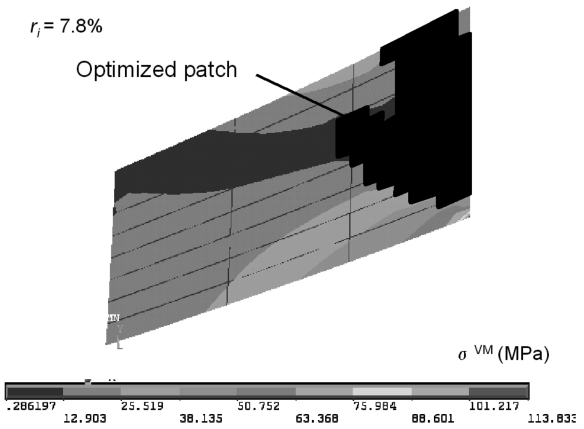

a) Aluminum patch

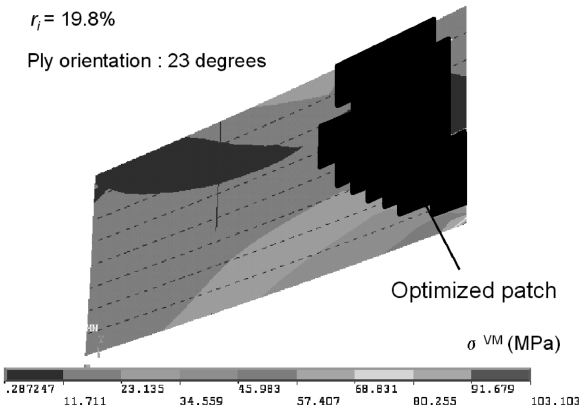

b) Boron patch

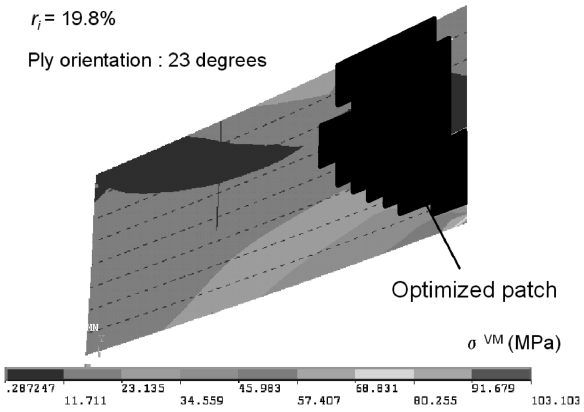

c) Quasi-isotropic carbon patch

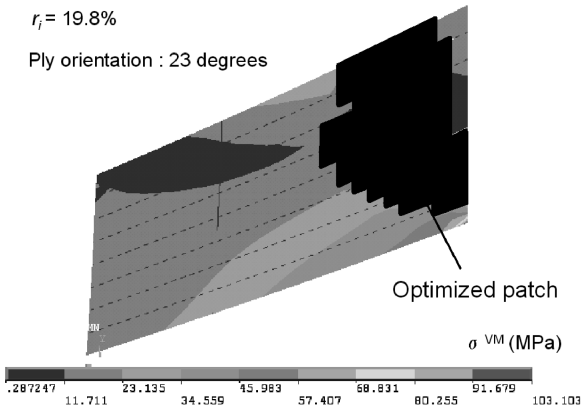

d) Quasi-isotropic boron patch

Fig. 9 Influence of the constitutive material.

These patches are made in aluminum and in quasi-isotropic carbon–epoxy and boron–epoxy laminates.

2) Area of the patch: The maximum allowable area of the patch A_p has been also changed. Composite patches have been optimized with a maximum allowable area which is successively equal to 15, 25, 30, 35, and 40% of the area of the patch A_w. In this case, the aim is to evaluate the influence of the area of the patch on the stress flow deviation.

3) Patch thickness: The thickness of the patch was finally modified. The initial thickness has been multiplied by 2, 0.5, and 0.25 to see the influence of the stiffness of the patch on the stress relief on the lower part of the wing.

B. Influence of the Material

In this section, many patches have been optimized with different materials: aluminum, composite patches made of boron–epoxy and carbon–epoxy plies, quasi-isotropic carbon–epoxy laminates, and quasi-isotropic boron–epoxy patches. The total thickness of the patch is 1.5 mm in all cases. Figure 9 represents results obtained. Several points are worth noting:

1) The shapes of the different patches are very similar to each other. The GA deviates the stress flow toward the upper right-hand part of the wing.

2) The shape of the aluminum patch is very similar to the shapes obtained with composite patches. The rating of the best aluminum

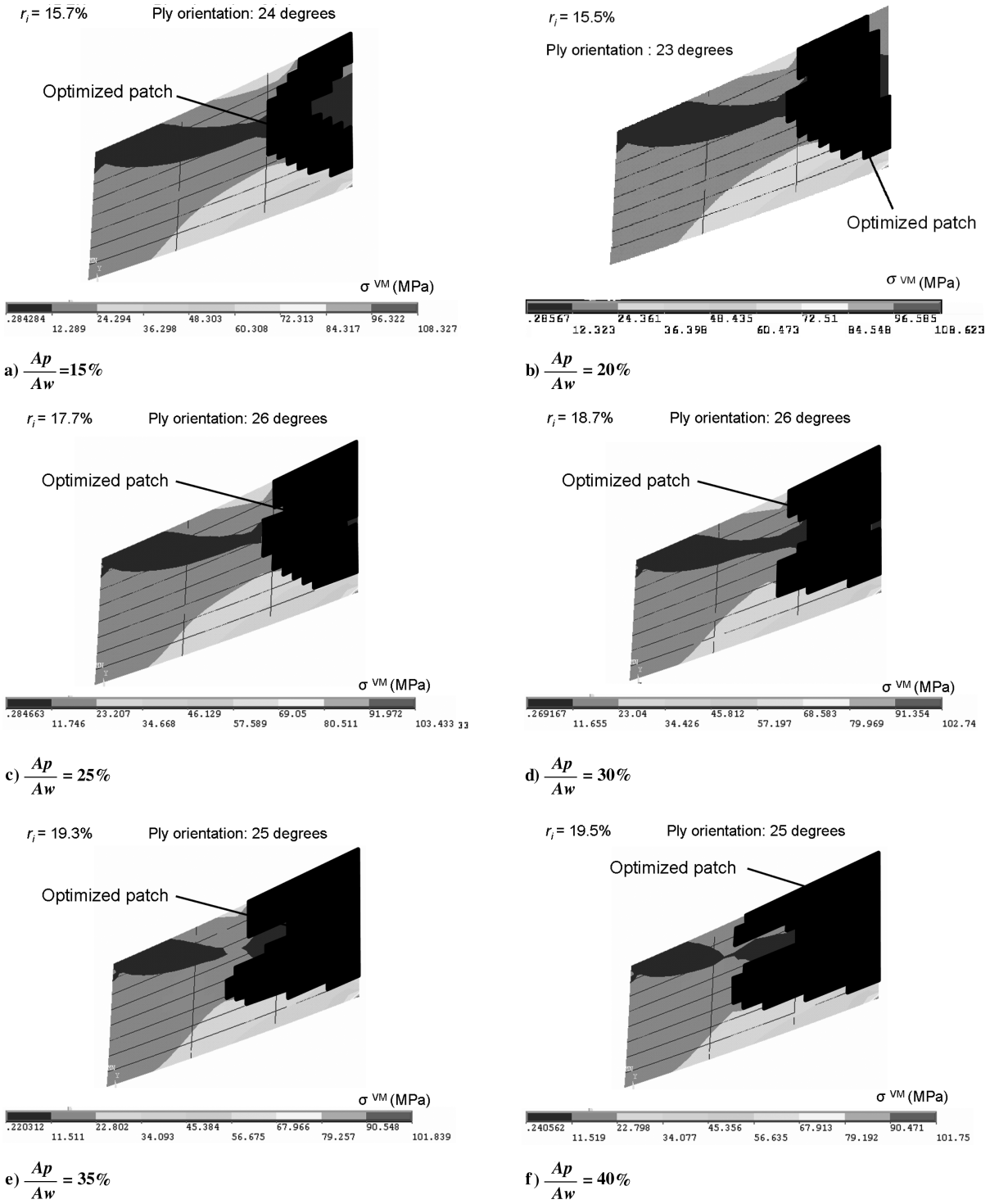

Fig. 10 Patches found for different maximum allowable areas.

patch is 7.8%, whereas the rating of the best carbon–epoxy composite patch is 15.5%. The best carbon–epoxy composite patch is twice as effective as the best aluminum patch for a given thickness. Using densities in [26], the carbon–epoxy patch (respectively, the boron–epoxy patch) is 1.8 times (respectively, 1.35 times) lighter than the aluminum patch. The weight of the latter would be equal to 4 kg. This underlines the relevance of using composite materials.

3) The boron–epoxy patch more or less exhibits the same shape as the carbon–epoxy patch and the ply orientation of all plies are equal. In this case too, they are nearly equal to the orientation of the stiffeners. The rating of the boron–epoxy patch is 19.8% instead of 15.5% for the carbon–epoxy patch. This better result is due to the greater longitudinal Young's modulus of the boron–epoxy unidirectional composite: 200 GPa instead of 141 GPa for the carbon–epoxy unidirectional composite (see Table 1).

4) The quasi-isotropic patches (carbon and boron–epoxy) exhibit the same shape as the aluminum patch. It is interesting to note that the quasi-isotropic boron patch is better than both the aluminum and the quasi-isotropic carbon patch (8.5% instead of 7.8 and 6.4%, respectively).

C. Influence of the Maximum Area of the Patch

The influence of the maximum allowable area A_p of the patch is examined here. If the patch area is very small, one can expect that the patch cannot deviate the stress flow in the structure. The same conclusion can be drawn if the area of the patch is high because the patch covers too large a part of the wing and cannot deviate the stress flow. It can easily be checked that a patch with an area equal to the structure area and fibers aligned with the stiffeners reinforces the damaged area with an efficiency equal to the ratio of rigidities that is about 5.5%. The following ratios between area of the patch and area of the wing have been analyzed: $A_p/A_w = 15$, 20, 25, 30, 35, and 40%. Figure 10 represents the optimized patches for these values. Several points are worth noting:

1) Any patch more or less includes the patch found with the immediate smaller area, thus meaning that the patch approximately expands from case to each other.

2) Shapes found with $A_p/A_w = 15$, 20, and 25% are very similar. Then, two main zones deviating the stress flow appear for the $A_p/A_w = 30$, 35, and 40% patches.

3) Figure 11 represents ratio r_i vs A_p. It is interesting to note that the curve converges to an r_i value equal to 20%.

4) A_p is in fact the maximum allowable area and it is interesting to note that the actual area of the optimized patches found in each case is very close to this corresponding maximum value.

D. Influence of the Patch Thickness

The influence of the patch thickness is considered in this section. The constitutive material is a carbon–epoxy composite. Thicknesses equal to 0.375, 0.75, 1.5, and 3 mm are considered. In these cases, the ratio r_i is respectively equal to 5.9, 9, 15.5, and 24.5%. Shapes and ply orientations found are the same in all cases: they correspond to the optimized patch represented in Fig. 7a. The composite patch deviates the stress flow toward the upper part of the wing. This trend is confirmed with different initial populations: the program always converges to solutions whose shape and location are similar to those of the best optimized patch.

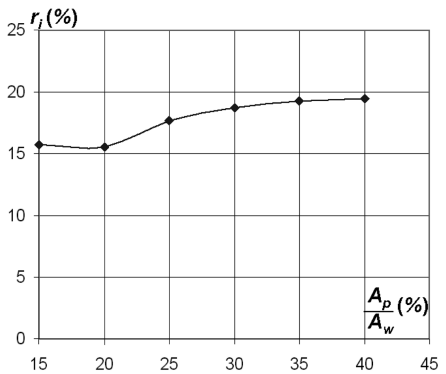

Fig. 11 Influence of the maximum allowable patch area.

E. Conclusion

At this stage, one can conclude the following:

1) The composite patch is nearly twice as efficient as the reinforcement of an aluminum patch of equal thickness.

2) Any patch more or less includes the patch found with the immediate smaller area when the maximum allowable area increases.

3) The shape, location, and ply orientations of optimized patches remain unchanged when the patch thickness is modified.

4) Optimized patches found in all cases never cover zone A to be relieved.

V. Conclusions

A genetic algorithm and a finite element code are used to optimize composite patches reinforcing wings. The shape of the patch and the ply orientations, as well as the location of the patch, are simultaneously optimized to define a patch which relieves a given area of the wing. The fitness function is computed with a finite element model developed under certain assumptions: perfect bonding between patch and substrate, two-dimensional model, and patch area limited to a given percentage of the wing area. Different examples are analyzed and the procedure provides results which cannot be guessed or obtained with some closed-form solutions. A sensitivity analysis was then carried out. The material, area, and thickness of the patch have been changed to evaluate the influence of these parameters on the solutions found. In all cases, one can observe the same strategy: optimized patches deviate the stress flow toward the upper part of the structure, thus relieving the damaged zone located in the lower part. It is finally interesting to note that optimized patches found in this study never cover the zone to be relieved.

Acknowledgement

The French Ministry of Defence is gratefully acknowledged for its financial support during this study.

References

[1] Baker, A., "Repair of Cracked or Defective Metallic Aircraft Components with Advanced Fibre Composites: An Overview of Australian Work," *Composite Structures*, Vol. 2, No. 2, 1984, pp. 153–181.
doi:10.1016/0263-8223(84)90025-4

[2] Baker, A., "Bonded Composite Repair of Metallic Aircraft Components: Overview of Australian Activities," AGARD CP- 550, 1995, pp. 1–14.

[3] Baker, A., "Bonded Composite Repair of Fatigue-Cracked Primary Aircraft Structure," *Composite Structures*, Vol. 47, Nos. 1–4, 1999, pp. 431–443.
doi:10.1016/S0263-8223(00)00011-8

[4] Baker, A., and Jones, R., *Bonded Repair of Aircraft Structures*, Martinus–Nijhoff, Dordrecht, The Netherlands, 1988.

[5] Riche, R. L., "Optimisation of Composite Structures by Genetic Algorithms," Ph.D. Thesis, Virginia Polytechnic Inst. and State Univ., 1994.

[6] Kogiso, N., Watson, L. T., Gürdal, Z., Haftka, R. T., and Nagendra, S., "Design of Composite Laminates by a Genetic Algorithm with Memory," *Mechanics of Composite Materials and Structures*, Vol. 1, No. 1, 1994, pp. 95–117.

[7] Kogiso, N., Watson, L. T., Gürdal, Z., and Haftka, R. T., "Genetic Algorithms with Local Improvement for Composite Laminate Design," *Structural Optimization*, Vol. 7, No. 4, 1994, pp. 207–218.
doi:10.1007/BF01743714

[8] Le Riche, R., and Haftka, R. T., "Improved Genetic Algorithm for Minimum Thickness Composite Laminate Design," *Composites Engineering*, Vol. 5, No. 2, 1995, pp. 143–161.

[9] Todoroki, A., and Haftka, R. T., "Stacking Sequence Optimization by a Genetic Algorithm with a New Recessive Gene Like Repair Strategy,"

Composites, Part B: Engineering, Vol. 29, No. 3, 1998, pp. 277–285. doi:10.1016/S1359-8368(97)00030-9

[10] Gürdal, Z., Haftka, R. T., and Hajela, P., *Design and Optimization of Laminated Composite Materials*, Wiley New York, 1999.

[11] Pedersen, P., "On Sensitivity Analysis and Optimal Design of Specially Orthotropic Laminates," *Engineering Optimization*, Vol. 11, Nos. 3–4, 1987, pp. 305–316. doi:10.1080/03052158708941053

[12] Mathias, J.-D., Balandraud, X., and Grédiac, M., "Applying a Genetic Algorithm to the Optimization of Composite Patches," *Computers and Structures*, Vol. 84, No. 12, 2006, pp. 823–834. doi:10.1016/j.compstruc.2005.12.004

[13] Kumar, A., and Hakeem, S., "Optimum Design of Symmetric Composite Patch Repair to Centre Cracked Metallic Sheet," *Composite Structures*, Vol. 49, No. 3, 2000, pp. 285–292. doi:10.1016/S0263-8223(00)00005-2

[14] Anthony, D. K., and Keane, A. J., "Robust-Optimal Design of a Lightweight Space Structure Using a Genetic Algorithm," *AIAA Journal*, Vol. 41, No. 8, 2003, pp. 1601–1604.

[15] Arizono, H., and Isogai, K., "Application of Genetic Algorithm for Aeroelastic Tailoring of a Cranked-Arrow Wing," *Journal of Aircraft*, Vol. 42, No. 2, 2005, pp. 493–499.

[16] Cho, M., and Rhee, S. Y., "Layup Optimization Considering Free-Edge Strength and Bounded Uncertainty of Material Properties," *AIAA Journal*, Vol. 41, No. 11, 2003, pp. 2274–2282.

[17] Murugan, S., and Ganguli, R., "Aeroelastic Stability Enhancement and Vibration Suppression in a Composite Helicopter Rotor," *Journal of Aircraft*, Vol. 42, No. 4, 2005, pp. 1013–1024.

[18] Wang, X.-L., and Shan, X.-X., "Shape Optimization of Stratosphere Airship," *Journal of Aircraft*, Vol. 43, No. 1, 2006, pp. 283–286.

[19] Van, K. D., Griveau, B., and Message, O., "On a New Multiaxial Fatigue Limit Criterion: Theory and Application," *Biaxial and Multiaxial Fatigue, EGF3*, Mechanical Engineering Publ., London, 1989, pp. 479–496.

[20] Hollaway, L., and Leeming, M., *Strengthening of Reinforced Concrete Structures*, Woodhead Publishing, Ltd., Cambridge, England, U.K., 1999.

[21] Lin, C. Y., and Hajela, P., "Genetic Algorithms in Optimization Problems with Discrete and Integer Design Variables," *Engineering Optimization*, Vol. 19, No. 4, 1992, pp. 309–327. doi:10.1080/03052159208941234

[22] Imam, M. H., and Al-Shihri, M. A., "A Primitive Crossover for Improving the Reliability of Genetic Algorithms for Structural Optimization," *Computational Engineering Using Metaphors from Nature*, edited by B. Topping, Civil-Comp Press, Edinburgh, 2000, pp. 91–97.

[23] Widagdo, D., and Aliabadi, M. H., "Boundary Element Analysis of Cracked Panels Repaired by Mechanically Fastened Composite Patches," *Engineering Analysis with Boundary Elements*, Vol. 25, No. 4, 2001, pp. 339–345. doi:10.1016/S0955-7997(01)00026-1

[24] Bouiadjra, B. B., Belhouari, M., and Serier, B., "Computation of the Stress Intensity Factors for Repaired Cracks with Bonded Composite Patch in Mode 1 and Mixed Mode," *Composite Structures*, Vol. 56, No. 4, 2002, pp. 401–406. doi:10.1016/S0263-8223(02)00023-5

[25] Tay, T. E., Chau, F. S., and Er, C. J., "Bonded Boron–Epoxy Composite Repair and Reinforcement of Cracked Aluminium Structures," *Composite Structures*, Vol. 34, No. 3, 1996, pp. 339–347. doi:10.1016/0263-8223(95)00159-X

[26] Gay, D., *Matériaux Composites*, Hermes, Paris, 1997.

A. Messac
Associate Editor